Cell-to-Module (CTM) Analysis for Photovoltaic Modules with Shingled Solar Cells

Max Mittag, Tobias Zech, Martin Wiese, David Bläsi, Matthieu Ebert, Harry Wirth

Fraunhofer Institute for Solar Energy Systems, Heidenhofstr. 2, 79110 Freiburg, Germany

***Abstract* — The interconnection of solar cells by shingling increases the active cell area in photovoltaic modules. Cell-to-module (CTM) gains and losses change significantly. We present models to calculate these gains and losses for shingled cells. Module efficiency and power can be increased with the shingle interconnection technology by +33 Wp and +1.86%$_{abs}$ in the analyzed design, when compared to common ribbon-based interconnection. While the CTM-ratio for efficiency improves due to shingling, the CTM-ratio for power is lower than for conventional modules with ribbon or wire cell interconnection.**

***Index Terms* — CTM, cell-to-module, shingle interconnection, efficiency analysis, photovoltaic module, concepts, modelling**

I. Introduction

The integration of solar cells into photovoltaic modules changes power and reference area which define the efficiency of solar devices. Those changes are caused by optical, electrical and geometrical effects and usually lead to a module power different from the sum of the solar cells' initial power [1]-[3].

The cell-to-module power ratio (CTM$_{power}$) describes the ratio of the power of the module after integration of the solar cells relative to the sum of the initial power of the solar cells before interconnection and module integration.

The individual CTM effects influence each other and render the optimization of the photovoltaic module a non-trivial task. This optimization is nonetheless necessary to further increase the performance of PV modules and to avoid unnecessary losses caused by an unfavorable combination of module components such as encapsulation material, interconnector ribbons or cover materials.

Electrical cell interconnection of common industrial modules relies on ribbons that connect the n-contact of one cell with the p-contact of the next cell. The interconnection concept of cell shingling [4]-[6] omits ribbons and directly connects stripes of solar cells (Figure 1). By doing so, the ribbons as well as the stringing process become redundant. The efficiency of the module increases since the cell spacing area is avoided, resulting in a higher share of active cell area within the module.

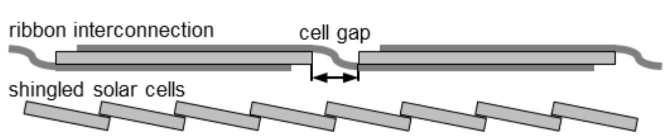

Fig 1: Ribbon based cell interconnection and shingled solar cells

Previous work [7] describes a unified methodology to analyze the CTM ratio of photovoltaic modules. Based on this approach we present new models for shingled cells.

Models for shingled solar cells differ from existing models for conventional cell interconnection since the shingling process actually reduces active cell area due to partial cell overlap. The total cell area for conventional modules is always smaller than the module area. For shingled modules, the initial cell area can be larger than the final module area.

We analyze the CTM gain and loss factors for shingled modules and present a detailed model for calculation of power and efficiency based on material properties and the specific module setup. The models are integrated into Fraunhofer ISE's software package SmartCalc.CTM [8], a recently released flexible, precise and user-friendly calculation tool.

II. Cell-to-Module Ratio Calculation

A. General model

A model to categorize the single CTM-factors and match them with physical loss mechanisms as well as with module components and layers has been presented in previous work and literature [7][9][10]. We use these models and calculate the module power P_{module} from the CTM-factors k and the sum of the initial solar cell power:

$$\mathrm{P}_{\mathrm{module}} = \prod_{i=3}^{m} k_i \cdot \sum_{j=1}^{\mathrm{n}} \mathrm{P}_{\mathrm{cell},\mathrm{j}} \tag{1}$$

$$\mathrm{C}TM_{power} = \prod_{i=3}^{m} k_i \tag{2}$$

We further extended this model and use it to describe the CTM-ratio of shingled modules and discuss relevant factors in the following section.

Figure 2 shows results of a CTM efficiency analysis for a conventional module considering 15 different gain and loss factors.

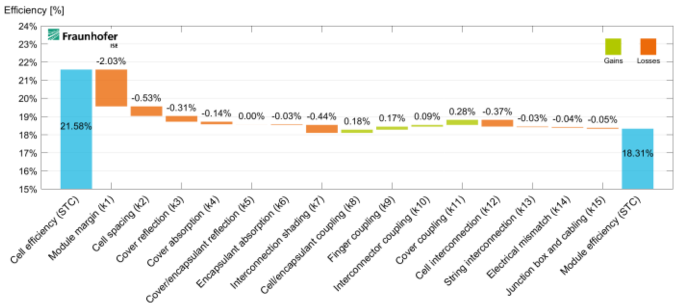

Fig. 2: Cell-to-module (CTM) loss and gain factors for a conventional photovoltaic module

B. Cell-to-module gain and loss factors for shingled modules

Losses by the inactive module margin and the cell and string spacing areas are described by factors k_1 and k_2. They account for geometrical losses of inactive areas that do not contribute to module power but influence efficiency. The latter can be calculated by:

$$\eta_{\text{module}} = \frac{P_{\text{module}}}{E_{STC} \cdot \left(A_{margin} + A_{cell\ spacing} + A_{cells}\right)} \tag{3}$$

$$\eta_{\text{module}} = \overline{\eta}_{\text{cell}} \cdot \left(k_1 + k_2 - 1\right) \cdot \prod_{i=3}^{m} k_i \tag{4}$$

The efficiency depends on the inactive module area which consists of module margin and cell spacing. The gap between cells in a string and the distance between different strings define the cell spacing area.

Models for factor k_1 (module margin) do not change for shingled modules. We therefore refer to Hädrich [7] who presents a detailed description of this factor.

Changes in k_2 (cell spacing) result from omitting the gaps between cells in a string. String spacing still exists. The factor k_2 describes the geometrical overlap and can be interpreted as the module area that can be saved by shingling.

$$k_2 = 1 + \frac{A_{overlap}}{A_{module}} \tag{5}$$

If shingling not only covers initially inactive (metallized) cell area but also some active cell area, the power loss from this shading is considered in factor k_7 (interconnection shading). In this case the mere geometrical factor k_2 overestimates efficiency gains. A change of cell spacing also affects the gains from reflection on the module rear cover (k_{11}).

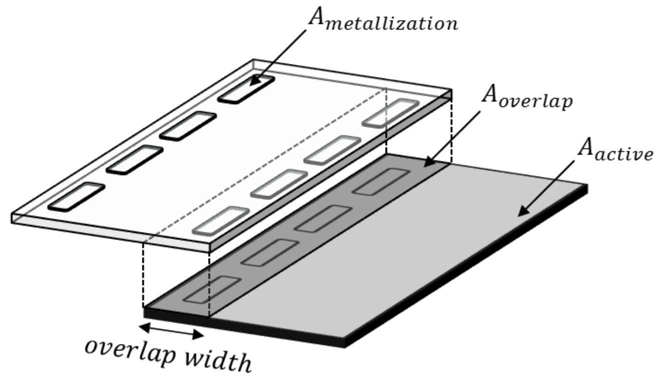

Fig 3: shingle interconnection of two cells with shaded area on the bottom cell ($A_{overlap}$)

Factors k_3, k_4, k_5 and k_6 describe the optical behavior (reflection, absorption) of the encapsulation bulk and do not change for shingled modules.

Changes occur in the modelling of shading by cell interconnection elements (k_7). Shading by interconnector ribbons does no longer occur but instead shading of the lower cell by the upper cell due to interconnection (Figure 3).

The shaded area usually does not only consist of inactive metallization area but also of active area. Therefore, the power output and the current of the lower cell are reduced. We thus use the area shares to calculate k_7:

$$k_7 = 1 - \frac{A_{overlap} - A_{metallization}}{A_{cell} - A_{metallization}} \tag{6}$$

Strings of shingled solar cells have to be interconnected within a module. Our model assumes that the shading of the string connector ribbon is the same as the cell overlap shading or that the gains of narrower ribbons can be neglected due to the mismatch losses of the shingled cells connected in series. Thus, we do not include the shading effects of string connector ribbons in k_7.

Factors k_8 (cell/encapsulant coupling) and k_9 (finger coupling) remain unchanged compared to other module concepts. The factors describe gains from optical coupling of solar cells after encapsulation.

Reflection gains from interconnector ribbons do not occur due to the absence of these ribbons. The corresponding factor k_{10} becomes unity. Again, we neglect the effects of string interconnection ribbons.

Factor k_{11} describes reflection gains from the rear cover of the module (usually a backsheet). Since a smaller share of backsheet area is visible in shingled modules, this factor is lower compared to conventional modules.

We perform measurements of the rear cover reflection gains using test equipment at Fraunhofer ISE. Results are displayed in figure 4.

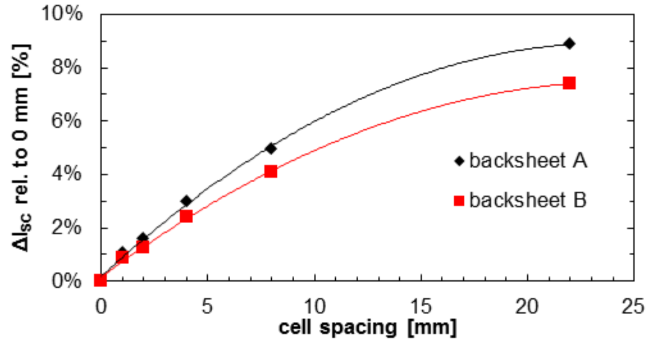

Fig. 4: I_{SC} gains of conventional solar cells totally surrounded by reflective backsheet material for varying cell spacing

An exponential model is used to describe the gains from cell spacing of a cell in a conventional module (7). The parameters a, b and c are fitted to measurement values [7].

$$I_{SC\,gain} = a \cdot \exp\left(\frac{\text{cell distance}}{b}\right) + c\,. \qquad (7)$$

Measurements are performed using full-size solar cells which feature four active cell edges in a conventional module setup. Cells for shingled modules can be manufactured by splitting full-size cells and cells in a shingled string only feature two active edges that can receive reflected light from the backsheet.

While cover reflection gain data for full-size cells is available, data for shingled cells is rare. We determine the effect of the active edge length on the coupling gain and calculate a corrected rear cover coupling for shingled cells.

Measurements to evaluate the effect of active edges are performed using cells that are partially shaded. This allows the variation of active cell edge. Results are displayed in figure 5.

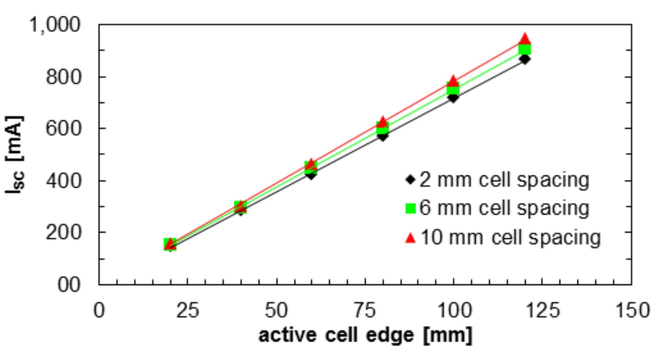

Fig. 5: I_{SC}-measurement results of solar cells with different active edge lengths, cells are shaded to cover parts of the cell edge and cell area, backsheet B.

We find the gains from rear cover reflection to be linear dependent on the active cell edge length. A correction of the I_{SC} gain of a full size cell is performed to fit shingled cells (8). The gain is corrected according to the active cell edge length of a cell in a shingled string.

$$\frac{I_{SC\,gain\,shingle}}{I_{SC\,gain}} = 1 - \frac{2 \cdot (\text{overlap width} + \text{cell width})}{\text{total cell edge length}} \qquad (8)$$

The calculation of the cover reflection gain k_{11} is then possible:

$$k_{11} = I_{SC\,gain} \cdot \frac{\text{active edge length}_{\text{shingled cell}}}{\text{edge length}_{\text{full-size cell}}} \qquad (9)$$

The end of each shingled cell string features a cell that has an increased active cell edge and therefore profits from higher irradiation. However, we neglect this effect due to the resulting electrical mismatch.

This method can also be used to correct the rear cover reflection gain for pseudo-square cells or modules with different cell and string distances.

Factor k_{12} describes electrical losses in the cell interconnection. Ohmic losses in ribbons do no longer occur but cells are interconnected using electrical conductive adhesive (ECA). Bulk resistance (ρ_{Bulk}) and contact resistance of ECA ($\rho_{contact}$) have to be considered. Equation (10) shows the electrical resistance R of an ECA-interconnection:

$$R = \frac{\rho_{\text{Bulk}} \cdot \text{thickness}_{\text{ECA}}}{A_{\text{metallization}}} + 2 \cdot \frac{\rho_{\text{contact}}}{A_{\text{metallization}}} \qquad (10)$$

The electrical resistance and the current of the cell string can be used to calculate the power losses of each individual shingled cell. The loss factor k_{12} is the ratio of the loss power and the cell power:

$$k_{12} = 1 - \frac{\sum P_{\text{loss},k12}}{\sum P_{\text{cell}}} \qquad (11)$$

While for conventional modules the serial connection of cell strings is common, shingled modules require different module topologies [11]. Strings can be connected in parallel or in networks. Ohmic losses in the string interconnectors can be calculated and (11) can be used accordingly to calculate k_{13}.

The current in a conventional module featuring serial cell and string interconnection is fixed and can be used for all cells. Since cells and strings may deviate regarding electrical properties, for parallel string interconnection the current of every string has to be used and losses have to be calculated separately.

Effects of variations in electrical parameters of cells and strings are considered in k_{14} (electrical mismatch).

Bins of cells feature inherent electrical deviations which lead to electrical mismatch. Cells for shingled modules are usually separated out of larger cells and electrical differences between solar cells may result from the separation of inhomogeneous full-size cells. Since these cells are electrically connected, mismatch occurs.

Also, the layup and interconnection process of shingled modules is related to inaccuracies which lead to different shading or variations in electrical cell parameters. This again results in losses due to electrical mismatch.

The precision of the cell layup is crucial for mismatch losses in shingled modules since differences in overlap (fig. 6) result in different shading. The shading results in different currents which lead to increased electrical mismatch of cells in strings.

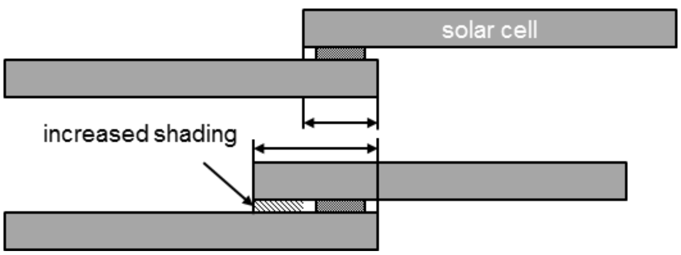

Fig. 6: Increased shading of shingled solar cells due to variations in cell placement during manufacturing.

Again, we use (11) to calculate the k-factor. The loss power for k_{14} is:

$$P_{loss} = \Delta P_{cell\ binning} + \Delta P_{cell\ separation} + \Delta P_{manufacturing} \quad (12)$$

Losses in junction boxes and cabling are considered in k_{15}. Despite the consideration of a possible change in the number of junction boxes and bypass diodes resulting from a different module topology in shingled modules (i.e. parallel string interconnection), no changes in the modelling of k_{15} are necessary for shingled modules.

All models described above are integrated into the SmartCalc.CTM software [8]. We use this software to perform an analysis of shingled modules.

III. CTM-Analysis of Shingled Modules

A. Simulation Setup

Input parameters for the CTM-analysis are determined at Fraunhofer ISE from commercially available module materials by measurements or datasheet analysis. The module we analyze features a low-iron glass with anti-reflective coating and 3.2 mm thickness. The encapsulant foil has a thickness of 0.45 mm and a low UV cut-off. The backsheet is white TPT. For the shingled module we assume a thickness of the ECA of 50 µm with a specific resistance of 0.1 Ωmm²/m.

The monocrystalline shingle cells have a size of 156.75 x 26 mm² and an efficiency of 21.6% (0.88 Wp). We assume a simple busbar metallization on front and rear side with a width of 0.8 mm.

Module dimensions are set to be 1667 x 998 mm (1.66 m²) with margins of 33 mm (top, bottom) and 23.75 mm (left, right).

We assume a cell overlap of 1 mm. Therefore, we receive 64 cells per string using the given module dimensions. String distance is 2 mm and we use 6 strings.

B. Results of the CTM-Analysis for Shingled Modules

The sum of initial cell power is 337.9 Wp. After performing a CTM-analysis with SmartCalc.CTM we find the module efficiency of the shingled module to be 20.2%. Detailed results are displayed in figure 7.

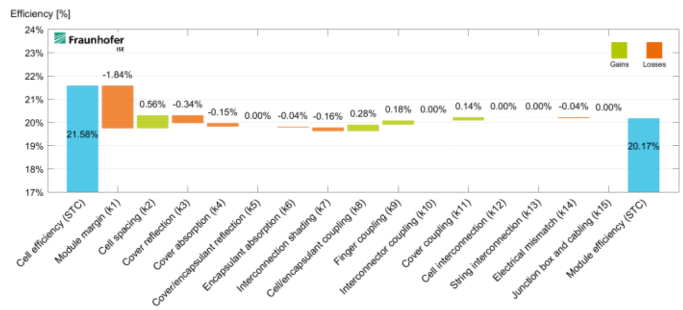

Fig. 7: CTM-analysis (efficiency) of a shingled module

Since the initial cell efficiency was 21.6%, the CTM-ratio for efficiency is $CTM_{efficiency}$ = 93.5%. A major impact factor is the module margin. Other losses are of much lower magnitude or become zero for shingled modules.

The power of the shingled module is 335.8 Wp which results in a CTM_{power} of 99.4%. Detailed results of the CTM-analysis for power are displayed in Figure 8.

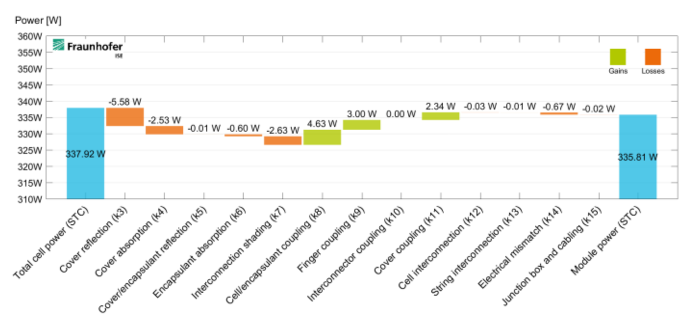

Fig. 8: CTM-analysis (power) of a shingled module

C. Results of the CTM-Analysis for Conventional Modules

We compare the results of the shingled module with a CTM-analysis of a conventional module with ribbon interconnection.

The copper-based ribbons have a cross-section of 1.5 x 0.2 mm². Cell and string distance are set to be 2 mm and margins are adjusted (40.75 mm; 23.75 mm) to have the same module area. The shingled cells are exchanged with pseudo-square cells (diameter 210 mm) of the same efficiency as before (21.6%, 5.24 Wp, 5 busbars).

The CTM-analysis of the conventional module shows a resulting module power of 302.8 Wp (η = 18.3%). The detailed analysis is shown in Figure 2. The CTM ratios for power and efficiency are CTM_{power} = 96.3% and $CTM_{efficiency}$ = 84.8%.

D. Comparison of both Module Concepts

Since both analyzed module setups feature cells of the same efficiency, the same materials and both modules are of the same size, we are able to compare both interconnection concepts. The shingled module has a higher output power, efficiency and CTM-ratios for power and efficiency are higher compared to the conventional module.

The higher output power of the shingled module (+33.0 Wp, +10.9%) is possible due to an improved CTM_{power} but also because more cells can be integrated into the module (+23.5 Wp, +7.5% initial cell power).

An increase in module efficiency can be achieved with shingled modules. The analyzed shingle setup shows an increase of +1.86 $\%_{abs}$ in efficiency.

E. Sensitivity Analysis

We perform a sensitivity analysis using SmartCalc.CTM and evaluate the influence of the overlap. We sweep the overlap depth from 1 to 2 mm and keep all other parameters constant (module area changes due to fixed module margins). Results are shown in Figure 9.

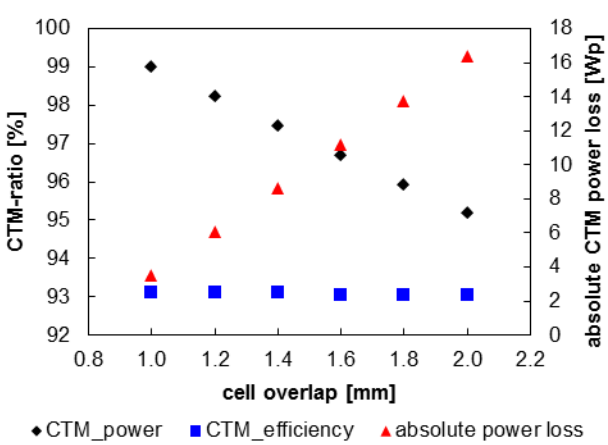

Fig. 9: influence of the overlap depth on CTM-ratios and absolute CTM power loss in shingled modules

We find the shingle overlap to be critical regarding the CTM_{power} ratio. Power loss due to overlap shading becomes a relevant factor for increased overlaps. Module efficiency is only slightly affected since only area shares are affected. The active area changes in size but its efficiency remains unchanged.

A tradeoff in overlap between manufacturing (cell layup precision) and costs (shaded cell parts do not generate power but have to be purchased/manufactured) needs to be achieved.

IV. Impact of Shingled Cells on Modules

Shingling solar cells is not only an alternative way of cell interconnection in PV modules, but also influences the design of photovoltaic modules. As mentioned earlier, the CTM ratios change but also module topology or module size can be affected.

Shingled modules currently feature cells that have approximately the size of 26x156 mm [12][13]. Due to the increased number of (smaller) solar cells in shingled modules, the module voltage increases if a conventional module topology that connects strings of solar cells in series (fig. 10, left) is used.

To be compatible with existing inverters and to not exceed system voltage limitations, electrical properties similar to conventional photovoltaic modules may be desired. Therefore, new module topologies featuring strings connected in parallel or combinations of parallel and serial cell and string interconnection are necessary and can be found in literature [12]-[15]. Shingling requires new solutions for string interconnection, junction boxes, and bypass diode placement. These changes have to be considered in CTM-analyses.

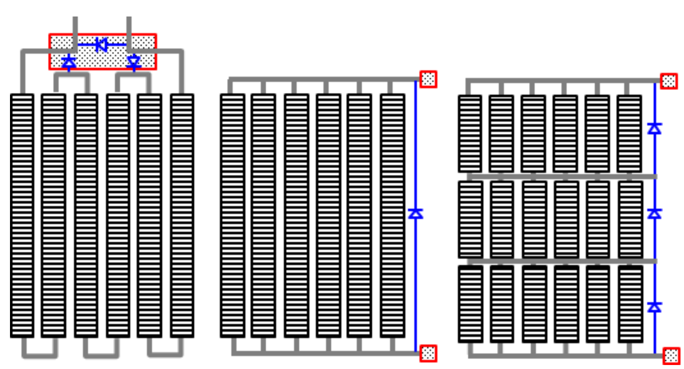

Fig. 10: different module topologies for shingled modules, left: conventional serial interconnection of strings, center: parallel interconnection of strings and two junction boxes, right: network of parallel interconnected strings with two junction boxes

The direct overlap of the cell stripes eliminates the cell gaps and therefore increases the active module area share. Two options are possible to use the resulting gains: A) keeping the module area constant and increasing power and efficiency or B) reducing the module size, keeping the module power constant and saving on module area and materials. We use the CTM-analysis of the conventional and the shingled module to analyze the benefits of both options.

Using the format of the conventional module (option A) and 26 mm shingle cells with 1 mm cell overlap, we are able to fit 64 shingled cells in a string. Module margins for the conventional module are increased (+6.75 mm on short module edges, compared to shingled module) to keep the dimensions of the module constant.

As presented above in the CTM-analysis of the shingled module, the module power is 335.8 Wp compared to 302.8 Wp of the conventional module (+33.0 Wp, +10.9% power in option A).

If we follow option B and reduce the module size, we only need 58 shingled cells per string and module power is calculated to be 304.3 Wp. The size of the module can then be reduced by 9.0%.

V. Summary and Conclusion

We extended an existing methodology to analyze the cell-to-module (CTM) losses and gains by developing new models for shingled cell interconnection. Models are presented and implemented into software. We use this software to perform a CTM-analysis of a shingled setup and compare the shingle concept with a conventional photovoltaic module.

Efficiency and power of the shingled module are higher than for the conventional module (+1.86%$_{abs}$, +33Wp). Also, the cell-to-module ratios for power and efficiency are improved for the shingled module.

We perform a sensitivity analysis of the overlap width and find it to be a crucial factor for CTM power losses in shingled modules.

We analyze a shingled module and a conventional module and find the power output of a shingled module can be increased by 10.9% compared to a conventional module of the same size. Shingled modules allow improved module efficiency.

References

[1] Singh, P. J. et al, "Cell-to-module power loss/gain analysis of silicon wafer-based PV modules", Photovoltaics International, 31st edition, 2016

[2] Peters, M. et al, "Full loss analysis for a multicrystalline silicon wafer solar cell PV module at short-circuit conditions", 29th PVSEC, DOI: 10.1002/pip.2593, Amsterdam, 2014

[3] Hanifi, H. et al, "Investigation of cell-to-module (CTM) ratios of PV modules by analysis of loss and gain mechanisms", Photovoltaics International 33rd edition, 2016

[4] "Photo-voltaic semiconductor apparatus or the like", patent US 2938938 A, 1960

[5] "Shingled array of solar cells", patent US 3769091 A, 1973

[6] Zhao, J. et al "Improved Efficiency Silicon Solar Cell Module", IEEE Electron Device Letters, vol. 18, NO. 2, 1997

[7] Haedrich, I. et al, "Unified methodology for determining CTM ratios: Systematic prediction of module power", Solar energy materials and solar cells 131 (2014), pp.14-23, ISSN: 0927-0248, SiliconPV, 2014

[8] www.cell-to-module.com

[9] Haedrich, I. et al, "PV Module efficiency analysis and optimization", PV Rollout, ISBN 9783941785-52-6, OTTI, 2011

[10] H. Wirth et al, "Photovoltaic Modules", ISBN 978-3-11-034827-9, DeGruyter,2016

[11] N. Wörle et al, "Solar Cell Demand for Bifacial and Singulated-Cell Module Architectures", Photovoltaics International 36th edition, 2017

[12] Sunpower Corp, "Sunpower Performance Series P17", technical product datasheet" 2016

[13] Jiangsu Seraphim Solar System Co., Ltd, "Eclipse", technical product datasheet, 2016

[14] R. Morad, G. Almogy, I. Suez, J. Hummel, N. Beckett, Y. Lin, D. Maydan, and J. Gannon, "Shingled solar cell module" US 14/605,695, November 1, 2016

[15] J. Zhao, A. Wang, E. Abbaspour-Sani, F. Yun, and M. A. Green, "Improved efficiency silicon solar cell module," IEEE Electron Device Lett, vol. 18, no. 2, pp. 48–50, 1997.